RSC Mechanochemistry

ROYAL SOCIETY OF CHEMISTRY

COMMUNICATION

View Article Online
View Journal | View Issue

Cite this: *RSC Mechanochem.*, 2026, **3**, 213

Received 23rd April 2025
Accepted 5th December 2025

DOI: 10.1039/d5mr00053j

rsc.li/RSCMechanochem

Encapsulation of (pseudo)halogen metal complexes in zeolite Y cages by mechanochemistry

Damjan Šinjori,†[a] Emilija Petrović-Hađar,†[b] Nikola Jakupec[c] and Ana Palčić *[c]

In an effort to introduce alternative methods of post-synthetic functionalization of zeolites, mechanochemistry was utilized for ion exchange and synthesis of transition metal halide and pseudohalide complexes within FAU-type zeolite cages. Structural characterization of the guest molecules shows a variety of synthesized compounds inside the zeolite cavities.

Zeolites are defined as microporous crystalline materials built of TO_4 (T = Si, Al, P, Ge, Ga, …) tetrahedra, forming well-defined 3D networks with channels and cavities up to 2 nm in diameter.[1] Their porous structure, tunable chemical composition, and chemical and (hydro)thermal stability enable enclosing molecules and usage as adsorbents, ion exchangers and catalysts.[2] Altering the properties of zeolite materials by post-synthesis modification procedures (*e.g.* ion exchange,[3] calcination,[4] delamination,[5] and grafting[6]) represents an additional advantage that can result in enhanced catalytic performance and higher separation (adsorption) capacity, as well as improved (hydro)thermal stability under certain conditions.[7]

Halogenides and pseudohalogenides (*e.g.* cyanides, CN^-) form complexes with transition metals (TMs) that have a wide range of applications owing to their stability in air and simple synthesis procedures.[8–15] CN^- complexes confined within zeolite cavities were prepared using a lengthy solution-based approach.[16–18] Such materials have been shown to bind gases, *e.g.* O_2.[16] Conversely, TM iodide complex synthesis in general, aside from triiodide compounds, has not been reported in detail so far, probably due to their dynamic equilibrium ($I^-/I_2/I_3^-$).[19]

Mechanochemistry represents an efficient way to mitigate the solubility and solvation issues in reactions in solution that often require high consumption of resources (*e.g.* solvents and energy). It was employed in post-synthesis modification of zeolites to further adjust their properties.[20–22] However, the synthesis of complexes within zeolite cavities has only been done in solution.[16–18,23–25] Herein, the preparation of (pseudo) halogen and transition metal complexes in the zeolite Y (ZY) void space was performed by mechanochemistry as a qualitative proof of concept. Furthermore, their mutual interactions were evaluated on the grounds of the phase composition of the materials exposed to atmospheres of corrosive gases.

TM complexes were mechanochemically synthesized in zeolite pores in two steps. First, the TM salts were milled with the Na form of ZY to exchange the Na^+ cations with TM cations (Ni^{2+}, Co^{2+}, Fe^{2+}, and Cu^{2+}) yielding the ion exchanged zeolite (ZY-M). KCN was added to ZY-M in the next step and milled once again to obtain the TM cyanide complexes (ZY-M-CN). Iodide complexes were produced analogously to the cyanide ones, using solid elemental iodine (I_2; ZY-M-I_2) and potassium iodide (KI; ZY-M-KI). The labels of the studied samples are listed in Table 1. In general, the zeolite framework is preserved after the second milling step, as shown by PXRD data (Fig. 1 and S1). In some cases, new peaks appear, suggesting the formation of a new phase detectable by PXRD, and in some, there are variations in the peak intensities, indicating disparity in the long-

Table 1 Samples prepared within the scope of this study. The ZY-M-CN and ZY-M-KI samples were washed with water, while ZY-M-I_2 samples were washed with ethanol

	I_2	KI	KCN
$FeSO_4 \cdot 7H_2O$	ZY-Fe-I_2	ZY-Fe-KI	ZY-Fe-CN
$Co(NO_3)_2 \cdot 3H_2O$	ZY-Co-I_2	ZY-Co-KI	ZY-Co-CN
$NiCl_2 \cdot 6H_2O$	ZY-Ni-I_2	ZY-Ni-KI	ZY-Ni-CN
$Cu(NO_3)_2 \cdot 3H_2O$	ZY-Cu-I_2	ZY-Cu-KI	Zy-Cu-CN[a]

[a] No cyanide compound obtained.

[a]Faculty of Science, Department of Chemistry, University of Zagreb, Horvatovac 102a, 10000 Zagreb, Croatia

[b]Division of Physical Chemistry, Ruđer Bošković Institute, Bijenička cesta 54, 10000 Zagreb, Croatia

[c]Division of Materials Chemistry, Ruđer Bošković Institute, Bijenička cesta 54, 10000 Zagreb, Croatia. E-mail: ana.palcic@irb.hr

† These authors contributed equally.

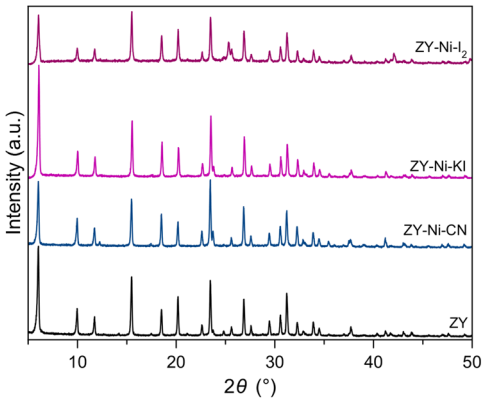

Fig. 1 PXRD patterns of the ZY-Ni samples milled with KCN/KI/I_2.

range ordering, potentially due to framework distortion, partial amorphization, local heterogeneity, *etc.* Furthermore, the energy dispersive X-ray spectra (EDS, Fig. S2) of selected Ni-containing samples suggest that there is a certain amount of Ni introduced into the zeolite crystals. The Na signals indicate that the ion exchange process was incomplete, consistent with the short duration of milling. Likewise, K signals in ZY-Ni-KI point to partial ion exchange with K occurring simultaneously with the formation of an I-containing complex compound.

Cyanide complexes were identified by comparing characteristic C≡N vibrations present in the mid-IR spectrum of the samples with the reference samples prepared *via* solution synthesis and the literature values (Fig. 2, S3, S4 and Table 2).[26] The Fe(II) system yielded hexacyanoferrate(II); $[Fe(CN)_6]^{4-}$. Reactions with Co(II) produced hexacyanocobaltate(III); $[Co(CN)_6]^{3-}$. Ni(II) containing reactions yielded tetracyanonickelate(II); $[Ni(CN)_4]^{2-}$, while reactions with Cu(II) did not yield a species containing a cyanide compound and will not be discussed further (Fig. S2). Considering that the polycyanometallate complexes are anions, it is assumed they are very likely accompanied by potassium cations (from the KCN) to balance out the charge since the zeolite Y framework is inherently negatively charged. Unlike cyanide complexes, iodine-containing compounds do not have discernible vibrations in the mid-IR range. They were identified *via* comparison of experimental far-IR spectra of the samples with calculated spectra obtained by DFT computational (Fig. 3) methods (functional: wb97xd, basis set: 3-21G*), since no literature mentioning the identified compounds exists, to the best of our knowledge. The system containing Ni(II) milled with KI yielded a new compound: potassium triiodonickelate(II); $K[NiI_3]$. When elemental iodine was used instead, dinickel(II) tridiodide cation, $Ni[NiI_3]^+$, another previously unknown moiety, was obtained. Far-IR spectra of the rest of the samples prepared from the systems containing I_2 or KI are shown in Fig. S4.

UV-Vis spectra of the solid samples with identified complexes were used as a reference in an attempt to identify the remaining compounds, which were not successfully simulated by DFT. Samples ZY-Cu-I_2 and ZY-Co-I_2 exhibit absorption maxima at 336 nm and 408 nm as seen in the spectrum of ZY-Ni-I_2 (Fig. 4a), pointing to species similar to $Ni[NiI_3]^+$ being present in the zeolite cages, possibly $Cu[CuI_3]^+$ and $Co[CoI_3]^+$, respectively. ZY-Fe-I_2 did not exhibit any band at 409 nm as ZY-Ni-I_2, and it lacks the absorption maximum at 336 nm, giving an inconclusive result. ZY-Fe-KI, ZY-Co-KI and ZY-Ni-KI share almost no similarities with ZY-Cu-KI (Fig. 4b) which seems to exhibit absorption maxima at an analogous position to that in ZY-Ni-I_2, indicating that the product is analogous to the one in ZY-Cu-I_2 (possibly $Cu[CuI_3]^+$). ZY-Fe-KI, ZY-Co-KI and ZY-Ni-KI have no discernible absorption maxima comparable to the identified moieties, so the identification of the species formed in these samples will be a subject of further study.

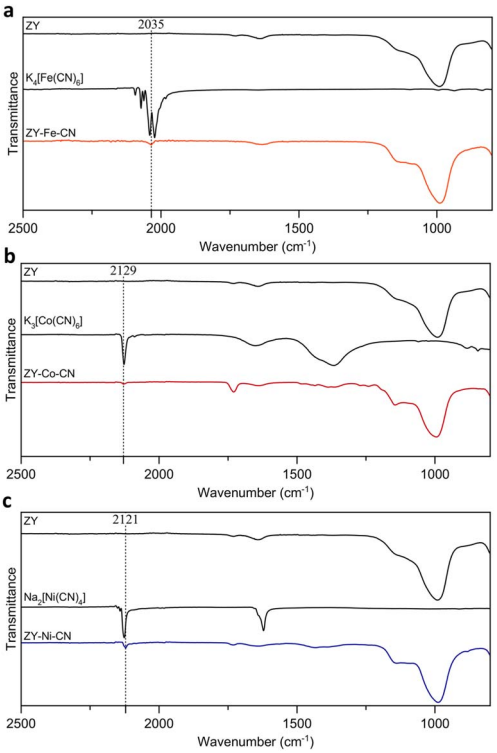

Fig. 2 Infrared spectra of the obtained samples compared to reference samples to identify formed polycyanometallate species inside zeolite cavities. (a) System containing iron(II). (b) System containing cobalt(II). (c) System containing nickel(II).

Table 2 Measured IR C≡N vibration values of the obtained samples compared to reference and literature values

	ν_{exp} (cm^{-1})	ν_{ref} (cm^{-1})	ν_{lit} (cm^{-1})[26]
$[Fe(CN)_6]^{4-}$	2035	2038	2037
$[Co(CN)_6]^{3-}$	2129	2129	2131
$[Ni(CN)_4]^{2-}$	2125	2122	2121

The stability of materials under given conditions affects their performance, so herein was evaluated the behaviour of the studied composite materials (zeolite-TM complex) upon being exposed to the atmosphere of acidic gases, since gas adsorption is one of the major application fields of zeolites, often the streams comprise acidic gases.[27,28] Exposure to corrosive

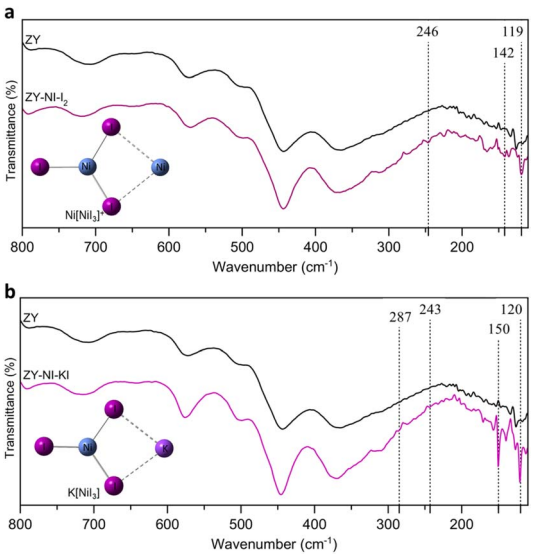

Fig. 3 Identification of iodide products *via* comparison of experimental far-IR spectra with calculated values. (a) Identification of Ni $[NiI_3]^+$. (b) Identification of $K[NiI_3]$. The vertical lines denote vibrations present in the simulated spectra.

atmospheres of hydrogen chloride (HCl) and nitrogen dioxide (NO_2) lasted for an hour, after which the samples were immediately analysed by IR and solid-state UV-Vis spectroscopy to confirm the presence of adsorbed gases/species. PXRD and scanning electron microscopy (SEM) were used to assess the impact on the zeolite structure and the surface of the particles. The IR spectra display vibrations corresponding to the vibrations of HCl (Fig. 5a, S6, S7 and Table S2) and NO_2 (Fig. 5c, S8, S9 and Table S2), even a month upon exposure in all cases, which strongly suggests that the gases form strong interactions with the studied zeolites. The appearance of multiple absorbance maxima at 225 nm and 292 nm in the UV-Vis spectra of the samples exposed to NO_2 (Fig. S10) in most samples (ZY-Fe-NO_2, ZY-Fe-KI-NO_2, ZY-Fe-CN-NO_2, ZY-Co-NO_2, ZY-Co-I_2-NO_2, ZY-Co-KI-NO_2, ZY-Co-CN-NO_2, ZY-Ni-I_2-NO_2, ZY-Cu-NO_2, ZY-Cu-I_2-NO_2 and ZY-Cu-KI-NO_2) implies multiple binding modes of NO_2 molecules either to the zeolite (possibly intra- and/or extra-framework Al) and/or to the encapsulated transition metal complex. It is worthwhile to note that while the absorbance maximum at 225 nm is in all cases very well defined, the maximum at 292 nm varies between samples from barely noticeable (ZY-Co-NO_2, ZY-Co-CN-NO_2 and ZY-Ni-I_2-NO_2) to well expressed (ZY-Fe-NO_2, ZY-Fe-KI-NO_2, ZY-Fe-CN-NO_2, and ZY-Co-KI-NO_2). ZY-NO_2, ZY-Ni-NO_2, ZY-Ni-KI-NO_2 and ZY-Ni-CN-NO_2 have a single absorbance maximum at 225 nm, while ZY-Fe-I_2-NO_2 is the only sample with a single absorbance maximum at 295 nm. These results point to the possibility of different NO_2 bonding modes, dependent on the metal and/or moieties present within the zeolite cavities.

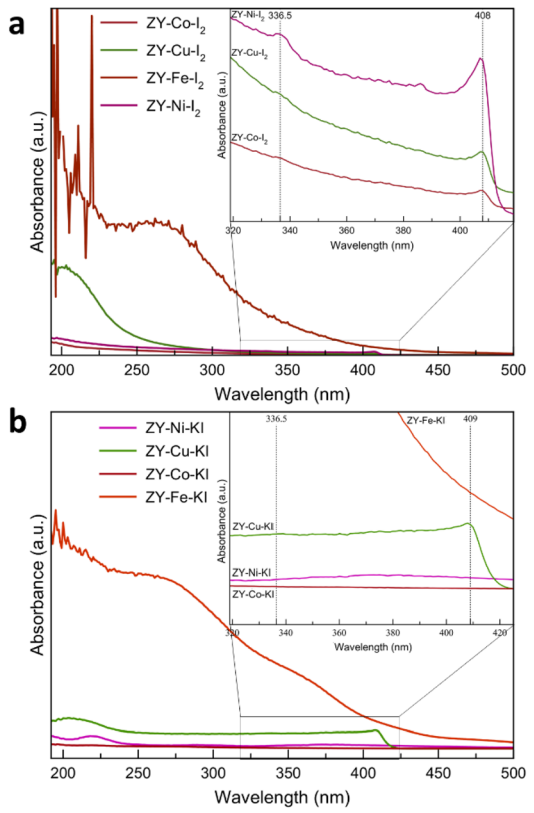

Fig. 4 Solid-state UV-Vis spectra of (a) ZY-M-I_2 and (b) ZY-M-KI samples (M = Fe, Co, Ni, Cu).

PXRD analysis after the exposure to the corrosive atmospheres shows a decrease in the peak intensities of the parent ZY (Fig. 5) indicating reduced ordering degree, most probably due to framework distortion and or/partial dealumination. A similar effect is observed in the ZY reflections of the TM complex samples (Fig. 5 and S11–S14), but to a smaller degree in NO_2 treated materials. On the other hand, after exposure to the corrosive atmospheres, individual crystals and their morphology can still be clearly discerned in SEM images (Fig. 5e). Furthermore, following the exposure to HCl, an additional phase begins to emerge from the parent ZY in PXRD (new peaks at 14.82°, 17.01°, 24.04°, 26.93°, 38.96° and 45.34°), whereas in the Ni-modified samples only peaks at 28.18° and 40.46° are observed. After one month, peaks of the unmodified zeolite Y are almost non-existent, while the Ni modified sample remains virtually unchanged with respect to the sample measured immediately upon the exposure to HCl. After exposure to NO_2, a new phase, besides FAU, is observed in the PXRD pattern of the parent zeolite Y (Fig. 5; additional peaks appear at 9.44°, 17.01°, 19.53°, 26.11°, 29.27° and 38.91°). After one month, a new set of peaks arises (at 13.34°, 14.08°, 19.66°, 21.66°, 22.10° and 38.82°), pointing to the formation of another secondary phase. Initially, the samples with complexes remain unchanged after the exposure to NO_2, but the very secondary phase as in the pure ZY is present one month after the exposure, pointing to the delayed phase transformation in the samples modified with TM complexes.

Samples containing (pseudo)halide compounds inside the cavities also show damage to the zeolite structure but to a lesser extent than the pure ZY. Therefore, it can be concluded that when exposed to acidic atmospheres, zeolites are stabilized by

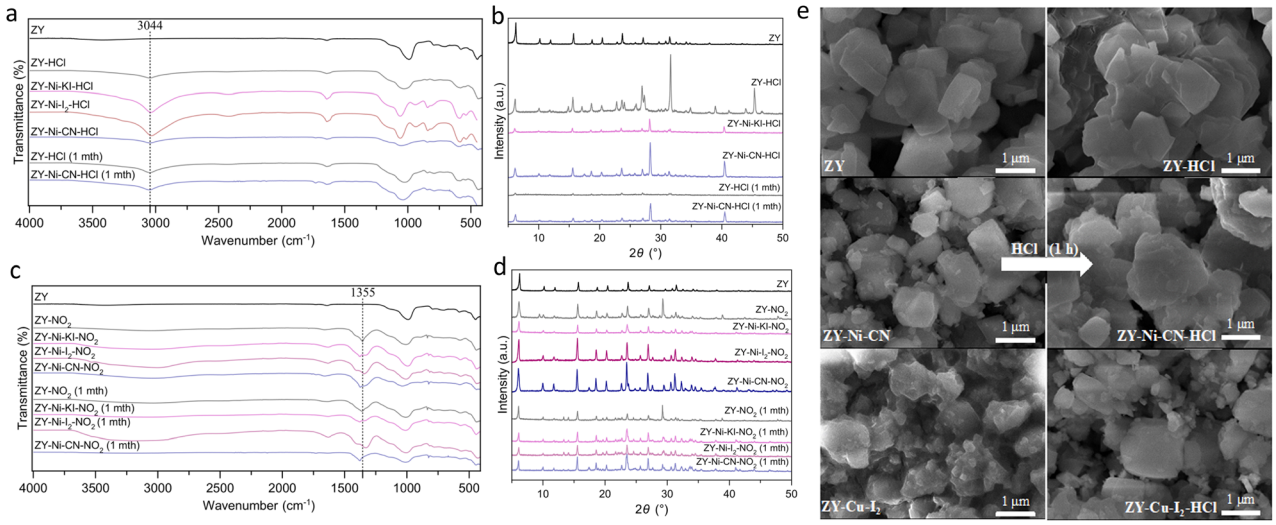

Fig. 5 Adsorption of corrosive gases by the modified zeolites. (a) IR spectra of samples exposed to HCl (g) for 1 hour, (b) PXRD difractograms of the same samples. (c) IR spectra of samples exposed to NO_2 (g) for 1 hour. (d) PXRD difractograms of the same samples. (e) SEM images of zeolite Y and samples modified with KCN and I_2 before and after exposure to HCl (g) for 1 hour. (mth = month).

transition metal (pseudo)halide complexes. This points to a stabilization effect of the FAU zeolite and the encapsulated complexes, where the zeolite stabilizes the compound inside the cavity and the compound stabilizes the zeolite against the effects of the corrosive atmospheres. The latter effect may be due to the compounds restricting access of gas molecules to the zeolite superstructure or other interactions being preferable, limiting potential framework changes caused by the corrosive gas. Finally, the particle size distribution (PSD) curves by number and volume (Fig. S15 and S16) suggest that the milling process dominates the particle size characteristics, while the chemical modifications introduce minor variations within the respective size distributions.

To sum up, zeolite Y was successfully mechanochemically modified with transition metals which were used to build halide (potassium triiodonickelate(II); $K[NiI_3]$, dinickel(II) triiodide cation; $Ni[NiI_3]^+$) and pseudohalide complexes (hexacyanoferrate(II); $[Fe(CN)_6]^{4-}$, hexacyanocobaltate(III); $[Co(CN)_6]^{3-}$ and tetracyanonickelate(II); $[Ni(CN)_4]^{2-}$) inside the zeolite Y cavities. This approach yielded new and previously unknown iodide complexes that are stabilized by the zeolite superstructure. In turn, the zeolite itself was more resistant to the corrosive effects of HCl and NO_2 due to the stabilization provided by the guest molecules. In the future, process parameters to increase the metal loading (*i.e.* the quantity of the formed TM complex species) will be optimized. This work opens a new avenue of research into mechanochemical transition metal complex synthesis inside zeolite cavities, especially synthesis of compounds that are unstable in air.

Conflicts of interest

There are no conflicts of interest to declare.

Data availability

The data supporting this article have been included as part of the supplementary information (SI). Supplementary information: materials and methods, additional PXRD diffractograms, UV-Vis and IR spectra, EDS spectra, and particle size distribution curves. See DOI: https://doi.org/10.1039/d5mr00053j.

Acknowledgements

This work was supported by the Croatian Science Foundation, project UIP-2019-04-4977. Marijan Marciuš is thanked for EDS results.

Notes and references

1 J. B. Nagy, P. Bodart, I. Hannus and I. Kiricsi, *Synthesis and Use of Zeolitic Microporous Materials*, DecaGen, Szeged, Hungary, 1998.
2 E. Pérez-Botella, S. Valencia and F. Rey, *Chem. Rev.*, 2022, **122**, 17647–17695.
3 R. P. Townsend and E. N. Coker, *Stud. Surf. Sci. Catal.*, 2001, **137**, 467–524.
4 J. Izumi and M. Suzuki, *Adsorption*, 2000, **6**, 23–31.
5 A. Corma, V. Fornes, S. B. Pergher, T. L. M. Maesen and J. G. Buglass, *Nature*, 1998, **396**, 353–356.
6 O. G. Nik, B. Nohair and S. Kaliaguine, *Microporous Mesoporous Mater.*, 2011, **143**, 221–229.
7 V. Valtchev, G. Majano, S. Mintova and J. Peréz-Ramírez, *Chem. Soc. Rev.*, 2013, **42**, 263–290.
8 D. G. Hottinger, D. S. Beebe, T. Kozhimannil, R. C. Prielipp and K. G. Belani, *J. Anaesthesiol. Clin. Pharmacol.*, 2014, **30**, 462–471.
9 G. B. Barton, J. L. Hepworth, E. D. McClanhan Jr., R. L. Moore and H. H. Van Tuyl, *Ind. Eng. Chem.*, 1958, **50**, 212–216.

10 D. F. Thompson, *Clin. Toxicol.*, 1981, **18**, 979–990.
11 B. Chen, J. Feng, Q. Chen, S. Xiao, J. Yang, X. Zhang, Z. Li and T. Wang, *npj Flex. Electron.*, 2022, **6**, 79.
12 S. Ghosh, *Bioorgan. Chem.*, 2019, **88**, 102925.
13 A. Chinnappan, D. La and H. Kim, *RSC Adv.*, 2013, **3**, 13324–13328.
14 S. Bougossa, N. Mhadhbi, A. Ben Ahmed, M. Hamdi, K. Elghniji, J. Erwann, K. Hamden, A. Oueslati and H. Naïli, *RSC Adv.*, 2024, **14**, 17413–17433.
15 K. R. Dunbar and R. A. Heintz, *Prog. Inorg. Chem.*, 1997, **45**, 283–391.
16 R. J. Taylor, R. S. Drago and J. E. George, *J. Am. Chem. Soc.*, 1989, **111**, 6610–6615.
17 L. A. Matkovskaya, Y. G. Gol'tsov, V. G. Voloshinets and V. G. Il'in, *Theor. Exp. Chem.*, 1996, **32**, 41–43.
18 Y. G. Gol'tsov, *Theor. Exp. Chem.*, 1999, **35**, 183–197.
19 D. A. Palmer, R. W. Ramette and R. E. Mesmer, *J. Solution Chem.*, 1984, **13**, 673–683.
20 K. Lázár, G. Pál-Borbély, H. K. Beyer and H. G. Karge, *J. Chem. Soc., Faraday Trans.*, 1994, **90**, 1329–1334.
21 Y. Huang, R. M. Paroli, A. H. Delgado and T. A. Richardson, *Spectrochim. Acta, Part A*, 1998, **54**, 1347–1354.
22 F. Martinovic, S. Ballauri, N. Blangetti, S. Bensaid, R. Pirone, B. Bonelli, M. Armandi and F. A. Deorsola, *Appl. Catal., A*, 2023, **658**, 119610–119618.
23 M. Salvati-Niasari, *J. Mol. Catal. A*, 2004, **217**, 87–92.
24 M. J. Alcón, A. Corma, M. Iglesias and F. Sánchez, *J. Mol. Catal. A*, 2003, **194**, 137–152.
25 K. Mori, K. Kagohara and H. Yamashita, *J. Phys. Chem. C*, 2008, **112**, 2593–2600.
26 A. G. Sharpe, *The Chemistry of Cyano Complexes of the Transition Metals*, Academic Press, Cambridge, 1976.
27 V. M. Georgieva, E. L. Bruce, M. C. Verbraeken, A. R. Scott, W. J. Casteel Jr, S. Brandani and P. A. Wright, *J. Am. Chem. Soc.*, 2019, **141**, 12744–12759.
28 E. Pérez-Botella, S. Valencia and F. Rey, *Chem. Rev.*, 2022, **122**, 17647–17695.